Journal of the Korea Institute of Applied Superconductivity and Cryogenics
Vol.10, No.2, (2008), pp.1~11

The recent investigation and engineering application of YBCO bulk materials

Z Hong, Y Jiang, R V Viznichenko and T A Coombs*

Cambridge University Engineering Deaprtment, Trumpington Street, CB2 1PZ, UK

***Abstract*-- The application of bulk superconducting materials to electrical power systems is very attractive because bulk high temperature superconductors offer excellent electromagnetic properties. In recent years there has been significant progresses in the research and fabrication of superconducting bulk materials. Numerous efforts have been made worldwide to make bulk YBCO as a replacement of the conventional magnets to produce larger magnetic field and hence to improve the device performance in electrical power applications. This paper gives a comprehensive review of different applications of bulk HTS materials, concentrating in three areas including superconducting bearing, superconducting motors and high field magnets. The advantages of applying superconducting material into each application are analysed. The status of current research in each section is summarized and examples are given to demonstrate how YBCO bulk materials can benefit the design of electrical devices. Several numerical models which calculate the electromagnetic properties of bulk superconductors are introduced and finally the article concludes with a review on the studies of the demagnetisation effect in superconducting bulk magnets which is extremely relevant to applying superconducting technology to rotating machines.**

1. INTRODUCTION

Since high-temperature superconductors (HTS) were discovered in 1986, there have been extensive research efforts to understand the nature of superconductivity in these materials and to fashion them into forms that can be used in practical applications. Bulk HTS materials, being attractive for their magical electromagnetic property of being able to trap magnetic field, is one of the most popular areas in HTS and have received significant amount of interest in recent decades. The current material of choice for most applications requiring HTS bulks are RE–Ba–Cu–O (ReBCO, RE denotes the rare earth elements) where Y–Ba–Cu–O (YBCO) is the most well known. These materials exhibit a high magnetic irreversibility field H_{irr} at liquid nitrogen temperatures and many have the ability to grow large grains. The H_{irr} marks a phase transition between the region where magnetic flux is solidly pinned in the superconductor and the region where flux may move. When compared with some of the members of the Bi, Tl or Hg HTS families, YBCO exhibits a relatively low critical temperature of 92 K, but its irreversibility curve is one of the highest at 77 K and lower temperatures. The potential of bulk melt-processed ReBCO single domains to trap significant magnetic field at 77K makes them particularly attractive for a variety of engineering applications, including superconducting magnets, magnetic bearings and motors. Machines made using these HTS materials will be smaller, lighter, and have higher power densities and efficiencies than existing machines. In most of the applications mentioned above, the full potential requires the HTS bulk to be used as trapped field magnets. The magnetization of the superconductor is proportional to the product of the critical current density (J_c) and the grain diameter[1]. Large grain diameters are important when sufficiently large magnetizations must be achieved for useful levitation forces. Therefore another reason that YBCO is the most popular HTS materials is that when bulk YBCO materials are made by a melt-texturing process, it is possible to grow grains to diameters of several centimeters[1]. In the present state of the technology, the upper limit of the grain diameter produced by this process is nearly 10 cm. The ability to produce good-quality YBCO thin films are also limited to approximately this size. The article proposed here reviews the development work in different areas to apply bulk YBCO materials into areas like magnetic bearings, electrical machines and superconducting magnets. Examples of ongoing studies will be given in each section to demonstrate how bulk YBCO materials can be utilized in engineering applications and improve current device performance. The numerical methods for solving the electromagnetic behaviour of bulk superconductors are summarized and finally the demagnetisation effect of bulk superconductors is discussed.

2. BEARING AND FLYWHEELS

Superconducting bearings are a major application for bulk HTS materials. The researches based on the design and fabrication of superconducting magnetic bearings have received continuous interest worldwide. There are two basic rotating bearing types: axial and radial bearings. In an axial bearing, the major load force is in the direction of the rotational axis, while in a radial bearing the load force is perpendicular to the rotational axis. A typical PM /HTS axial bearing configuration could consist of a fixed

* Corresponding author: tac1000@cam.ac.uk

shaft with HTS materials mounted as around it, and a rotating cylinder with permanent magnets (PMs) pattened on the inner surface. The PMs face the superconductors between a small air gap. The arrangement shown in figure 1 is an example of an axial bearing. In this review, the discussion focuses on the axial type. However, researchers have also demonstrated PM/HTS journal bearings[2, 3], and significant amount of results have been achieved. The most important parameters needed to characterize a bearing for use in rotating a mass are the levitational force, dynamic stiffness, damping, and rotational loss. Significant interest in superconducting bearings did not emerge until the discovery of the first HTS; major advantages of HTSs were their relatively simple fabrication and use in bulk form and a much higher magnetic field. The 280 kPa levitational pressure of an typical HTS bearing is lower than that achievable with a conventional electromagnetic bearing (1MPa) and significantly lower than that typically achieved with mechanical roller bearings (10MPa). Several laboratories have stably levitated and rotated masses larger than 200 kg. In principle, the amount of mass that can be levitated is limited only by the number and size of PMs and HTSs that are available.

In a superconducting bearing, the superconductor is not generally acting as a permanent magnet. Rather it is acting as the active element in an otherwise passive rare earth magnetic system. The principle which all superconducting bearing use is that the superconductor being strongly diamagnetic will mirror the field produced by a permanent magnet. The consequent repulsion produces levitational force and crucially whenever the magnet moves, losses in the superconductor which stablise the system allow a passive bearing with no active control to be produced.

HTS bearings have very low coefficients of friction and are ideal for flywheel energy storage. Several major projects have investigated this application [4-10]. Flywheels with conventional bearings typically suffer from high-speed rotational losses whereas, with HTS bearings, it is believed that losses can be scaled down to 10%, even when the flywheel powers the refrigerator that cools the HTSs. When coupled with efficient motors/generators and power electronics, the potential exists for constructing flywheels with a significantly high cycle efficiency. Probably only one other technology is capable of achieving such high storage efficiencies: large superconducting magnetic energy storage, which employs superconducting coils hundreds of metres in length.

Cambridge's team has done a significant amount of work in applying superconducting passive bearing to the flywheel energy storage system. For example, the project introduced in the following paragraph focused on using flywheels to support the electric train networks. The load imposed by a railway system onto the grid can be uneven, causing problems with supplies to other equipment. Also, modern rail vehicles have the ability to regenerate energy into the supply during braking. This is only possible if another load, such as an accelerating train, can take the energy; otherwise it will just be dissipated as heat in brake resistors. The addition of flywheels to such a system enables the peak demand to be supplied by the flywheel, thus smoothing out the load on the grid. Also, they can provide a permanently receptive supply for the brake energy that is subsequently transferred back into the steady-state load on the system.

This particular application is quite unlike, for example, the diurnal storage systems where the expectation would be that energy could be bought when cheap, stored in a flywheel, and then sold when energy is expensive, or, for that matter, power quality management systems where energy is stored in anticipation of short timescale dropouts. In both these applications there is a low level of cycling. In the electric train network, however, the cycle time can be as short as 90 s. This is significant because the principal competitor to a flywheel, i.e. a battery, has a lifetime which is determined by the number of cycles to which it is subjected. This paper will report on two aspects of the work being carried out. The first aspect is the experimental work and the second is the model which has been created to support the experimental work. This particular application is quite unlike, for example, the diurnal storage systems where the expectation would be that energy could be bought when cheap, stored in a flywheel, and then sold when energy is expensive, or, for that matter, power quality management systems where energy is stored in anticipation of short timescale dropouts. In both these applications there is a low level of cycling. In the electric train network, however, the cycle time can be as short as 90 s. This is significant because the principal competitor to a flywheel, i.e. a battery, has a lifetime which is determined by the number of cycles to which it is subjected. This paper will report on two aspects of the work being carried out. The first aspect is the experimental work and the second is the model which has been created to support the experimental work.

The flywheel system includes a superconducting bearing on the stator and a magnetic bearing on the rotor. The superconducting bearing consists of a nonmagnetic steel cryostat for liquid nitrogen which is fixed to the central shaft and a set of YBCO high temperature superconductors glued to the outer part of the cryostat as shown in figure 1. The outer diameter of the HTS bearing is 167 mm.

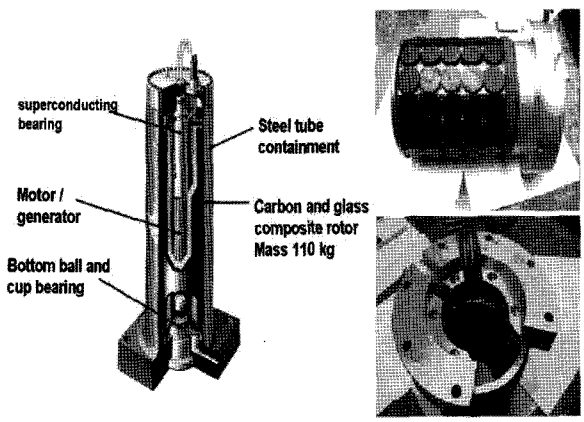

Fig. 1. The configuration of the flywheel and the superconducting bearing.

As the bearing works in vacuum chamber, it has rather good thermal insulation. To improve it further, tufnol spacers are used to avoid direct contact with metallic parts of the stator. Thermocouple based temperature monitoring is used to watch the temperature of the superconductors. 75 superconducting samples with thickness 5 mm and diameter 31 mm were required to build this bearing. A ring of permanent magnet is used to stabilize the rotor in a central position while the superconductors are above their critical temperature. The performance of the bearing is measured and the experiments have shown that bearing stiffness is affected by temperature variation, eccentric loading and vibration amplitudes during natural resonances.

The response of the bearing to cryogenic failures was studied and the results are showed in figure 2. It can be observed that the rotor goes through a broad resonance spread over 10Hz or more and up to three resonances before touching down at the critical transition temperature around 90K. During the resonance, the levitated rotor wobbles over the superconductor and this wobbling is similar to a magnet vibrating with a certain frequency over the superconductor. It is worth noting that the stiffness of the bearing decreases with increasing frequency. This decrease would be further amplified by the increasing temperature. Appearance of multiple resonances during warm up suggests a sudden change in the stiffness of the bearing. The investigations have shown that during a failure, the rotor goes through various modes of resonance induced by changing stiffness before it touches down. The frictional losses increase with the increase in rate of temperature change.

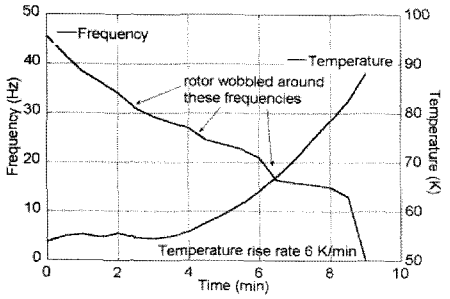

Fig. 2. The decrease of frequency against the temperature in cryogenic failure test.

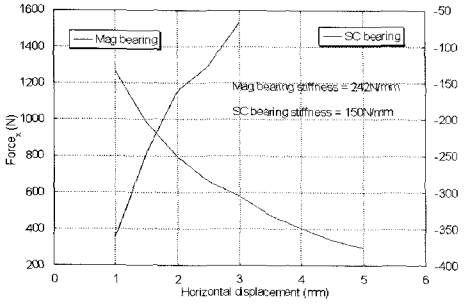

Fig. 3. Force-displacement curve for superconducting bearing and magnetic bearing.

Bearing stiffness and AC loss have been estimated using finite element modelling, which allows choosing the real 3D geometry and magnetic field configuration. The field-cooled superconductor is modelled as a diamagnet in respect to any changes of original external magnetic field. Magnetic field distribution, force *vs* displacement and stiffness of the bearing have been estimated. The results gives the value of stiffness at 140-180 N/mm for the top superconducting bearing in figure 3.

The operational AC loss of superconducting bearing has been calculated by numerical solver of critical state model [11, 12]. The result shows that critical currents flow only in a thin undersurface layer of the superconductor and screen the superconducting volume from external AC magnetic field (figure 4). The AC losses in the superconductor have been evaluated as ohmic losses and estimation shows that the superconducting bearing could damp 27-36 % of the total energy of parasitic vibrations. Thus, using the superconducting bearing will provide good stiffness and add an additional damping to the rotor.

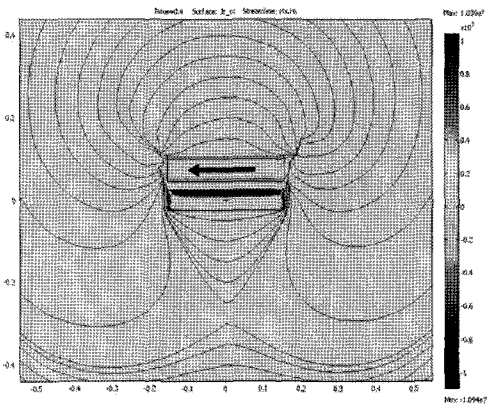

Fig. 4. Current distribution in a superconducting puck Induced by an external AC magnetic field.

3. MOTORS

The advent of high-temperature superconductivity has created the opportunity for a step change in the technology of large electric machines. HTS-based motors and generators will be smaller, lighter, more efficient, and less expensive to manufacture and operate than conventional machines. The potentially significant cost, size, weight and efficiency benefits of superconducting machines will change the dynamics of the electrical machinery industry. This unique situation leads to reduced manufacturing costs. The initial use for HTS motors will likely be in transportation applications, particularly naval and commercial ship (marine) electric propulsion, where critical size and weight savings will provide a key benefit by increasing ship design flexibility. HTS motors are ideal for use in pumps, fans, compressors, blowers, and belt drives deployed by utility and industrial customers, particularly those requiring continuous operation. These motors will be suitable for large process industries such as steel milling, pulp and paper processing, chemical, oil and

gas refining, mining, offshore drilling, and other heavy-duty applications. Most of the applications of motors and generators utilized superconducting coils to construct the rotor or stator. Until recently, bulk superconducting materials have been applied to the design and fabrication of superconducting motor. Jiang el. proposed a novel prototype of superconducting synchronous motor which uses superconducting materials for both stator and rotor: YBCO pancake coils are used on the stator and magnetized YBCO bulks on the rotor[13].

A schematic cross-sectional view of the HTS motor is shown in figure 5. The stator consists of the air gap HTS armature windings, which are installed in the slots of the nonmagnetic and insulating material, and an iron shield. The rotor is made of superconducting pucks, which can be magnetized and equate to a four-pole permanent magnet. The HTS motor is cooled by liquid nitrogen to 77 K.

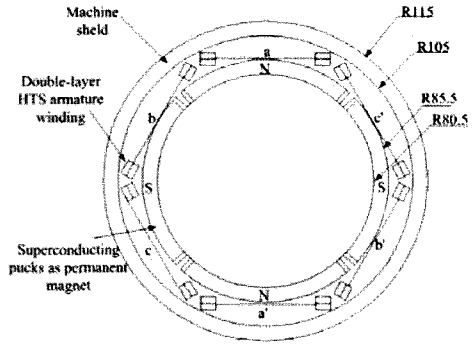

Fig. 5. Cross-sectional view of HTS permanent magnet synchronous motor.

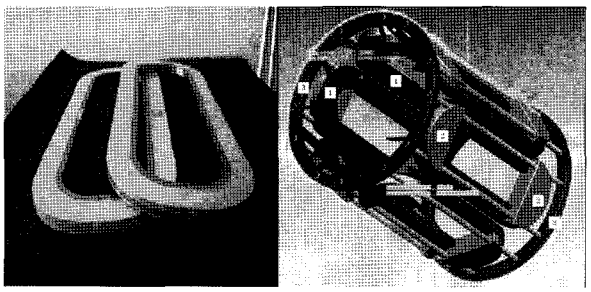

Fig. 6. Photo of two pancake windings and the construction of the motor stator.

Since the armature winding sees a rotating magnetic field, it has to be arranged to minimize the AC losses. In the design of the HTS armature winding, the magnetic field from the rotor is parallel to the tape in order to minimize AC losses [14]. Meanwhile, the YBCO tape is rather brittle having a maximum strain of 0.3%. Consequently, the armature winding in the HTS motor is made of six single flat-loop coils which are wound as racetrack coils with a bend radius of several centimeters. Racetrack windings and the geometry are shown in figure 6(left). Double layers of HTS windings are stacked together to make one racetrack winding, which doubles the number of turns of the winding, and maximises the inductance of the winding within the limited geometry. The total number of turns per phase for the stator windings is 200 turns, with 50 turns for each layer. The construction of the motor stator can be seen in figure 6(right). The stator of the HTS motor consists of six pancake HTS armature windings (labeled 1), non-magnetic supporters (labeled 2) to fix the windings' positions, and the non-magnetic outer rings (labeled 3). At a later stage, a machine shield will be applied to screen the electromagnetic radiation.

HTS pucks, acting as permanent magnets when magnetised, are adopted to construct the rotor. The configuration of the rotor is shown in figure 7. The rotor consists of a shaft in the middle made of nonmagnetic material, a shallow space to fill in liquid nitrogen to cool the superconducting pucks, and 75 round superconducting pucks which are attached on the copper wall by a 1 mm low temperature adhesive layer. The copper wall conducts the heat from superconducting pucks to liquid nitrogen. The rim of the rotor is made of thermo-insulated material. The total diameter of the rotor is roughly 180 mm. At the beginning of the machine operation, the armature HTS windings are used to generate the magnetization field for the rotor. Each one of the armature phases is supplied with a DC current in order to generate a static field, emulating the magnetic field produced by an alternating three-phase current system balanced at a given time. Then the rotor will be cooled by liquid nitrogen, and the pucks will become superconducting, which will hold the flux within. Afterwards, three-phase AC currents will apply to the stator, and the machine will act as a permanent magnet synchronous motor.

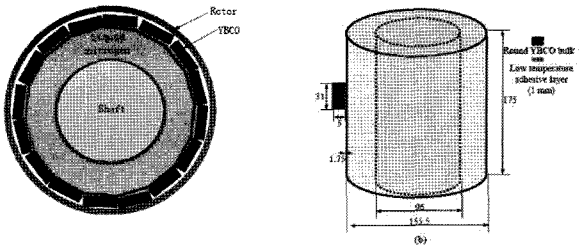

Fig. 7. Cross-sectional view and 3-D configuration of the rotor.

The magnetic field produced by the magnetized superconducting pucks is modeled by FEM and the strength is estimated to be 0.3 T. The critical current carried by the armature winding was measured to be 51A per phase. A generic control scheme especially designed for superconducting rotating machines is applied to this motor [15] and the performance of the machine is modeled by *Simulink*.

The calculation shows that the superconducting motor can deliver an electromagnetic torque at 100Nm with a rated power of 15.7kW.

4. NUMERICAL MODELLING

The investigation of the electromagnetic behaviour of superconductor, especially in critical state, is crucial to the

design of the devices using HTS materials. Many groups dedicated for decades for developing mathematical methods to solve the critical state analytically or numerically. Most of the proposed methods look for a macroscopic description of the electromagnetic phenomena in the material using Maxwell's equations. Analytical methods [16], [17] have been developed for simple geometries and uniform field conditions. For more complicated shapes and field conditions, numerical methods should be developed. These numerical models usually use the finite element method (FEM) or the finite difference method to solve Maxwell's equations in two dimensions or three dimensions. These methods can be classified by the main equations they use: A–V formulations, T–Ω formulations, and the unconstrained H-formulations.

A-V formulations have been selected frequently in the literature as the governing equations to solve the critical state in superconductivity. A-V formulations are derived from Maxwell's equations by introducing magnetic vector potential A as the state variable, coupled with the *E-J* constitute law.

$$\mathbf{E} = -\frac{\partial \mathbf{A}}{\partial t} - \nabla V \tag{1}$$

$$\nabla \times \frac{1}{\mu_0} \nabla \times \mathbf{A} = \mathbf{J} \tag{2}$$

where A is magnetic vector potential, **E** is electrical field, **J** is the current density and V is the electric scalar potential. Equations (1), (2) and *E-J* constitutive law make up of the framework of A-V formulations. Brandt's [17-19] method is one of the most popular numerical methods based on A-V formulation. He proposed a 2-D numerical solution to the current distribution of superconductors of finite thickness in perpendicular homogeneous magnetic field, with an exponential *E-J* constitutive law. This method was the first attempt to solve the critical state on the cross section of superconducting bulk. Prigozhin [16, 20, 21] gives solutions for the problem in the cases of 2-D, axially symmetric and thin film geometries. The method states a variational inequality problem to solve the current distribution inside the superconductor. The derivatives in time of this problem are approximated by a finite difference method to give a quasi-stationary problem. Then, the section of the superconductor is discretized in a finite element scheme and the problem is transformed into an equivalent energy minimization problem. Barnes [22-24] proposes a combined method to solve the current distribution in the superconductors embedded with other materials in 2-D problems. They assume quasi-static analysis of the problem, so for each time step they perform a static analysis of the superconductor in the system. They have an FEM solver for the system, considering the superconductor as a current distribution in air. This gives a magnetic field distribution in the superconductor region that is the input for another solver that finds the current distribution within the superconductor. The driving force of the superconductor is only the time-varying magnetic field. This is the input for the FEM solver in the next time step. Coombs [25, 26] proposed a fast numerical algorithm with an iterative scheme. It can be used for asymmetric samples in non-uniform fields. In this technique the sample starts with no current flowing. Elements carrying J_c are then inserted at the point of maximum vector potential and the field recalculated. The process is continued until the external field is screened from the interior. This model assumes that E and J are parallel. The excitation of the system is a change in A_e (external change of vector potential). The superconducting region is divided into elements. For each time step, a solution has to be found iteratively from Equation (3):

$$J = -\sigma(J)\frac{(A_i(J) + A_e - A_i(\hat{J}) - \hat{A}_e)}{\Delta t} - \sigma(J)\nabla V \tag{3}$$

Where J is calculated current density in every element and $\sigma(J)$ is the incremental value of current density in each element, without transport currents, $\nabla V = 0$. Then, in the element where $|A_e|$ is maximum, an incremental current is inserted. The new $A_i(J)$ and σ is calculated and the process is repeated until the initial disturbance is corrected. Notice that in this case, Δt doesn't affect the result of the algorithm since it is a constant and the method is interested only in finding the element where the absolute value of equation (3) is a maximum.

The numerical methods described above have the common characteristic of using A-V formulation as the governing equation. Hong [11] proposed a numerical solution to critical state based on a direct magnetic field H formulation without the use of vector and scalar potentials. In this numerical scheme, a set of Maxwell's equations have been adopted into a commercial FEM software (Comsol Multiphysics) to solve the critical state in superconductivity in two dimension. It is a flexible, extendable numerical method without an algorithm and can be simply implemented into most of the FEM software to get an easy solution to many problems in complex geometries. The governing equations are:

$$\nabla \times \mathbf{E} = -\mu_0 \mu_r \frac{\partial \mathbf{H}}{\partial t} \tag{4}$$

$$\nabla \times \mathbf{H} = \mathbf{J} \tag{5}$$

In a 2D problem there are two dependent variables: $\mathbf{H}=[H_x\ H_y]$, representing the components of the magnetic field in the x and y directions. The induced electric field and the current density only have the components perpendicular to the cross section of the sample. So $\mathbf{E}=E_z$ and $\mathbf{J}=J_z$. This method avoids using second-order derivatives in the partial differential equations which allows using first order elements in the FEM solver. This improvement significantly reduced the total number of elements required by an accurate solution. Additionally, the magnetic field variables are immediately available in the solution and they don't need to be calculated by differentiating the

magnetic vector potentials which might introduce some inaccuracy. Another benefit of using magnetic field components as state variables are very easy for imposing the boundary conditions. A Dirichlet boundary condition can be set up as: $H_x=f_x(t)$ and $H_y=f_y(t)$, Where $f_x(t)$ and $f_y(t)$ are functions that describes how the external field in the x and y directions vary with time. This method is further improved by Brambilla [27] who introduce edge-element to the solver. This improvement allows the overcoming of one of the major problems of standard nodal elements with potential formulation: in the case of strong discontinuities or nonlinearities of the physical properties of the materials, the discontinuities of the potentials' derivatives are unnatural and without smoothing artifices the convergence of the algorithm is put at risk. Many commercial FEM modelling packages have been used as numerical platform for modelling superconductivity.

All the equation based models of critical state have to compromise to use nonlinear *E-J* power law with a large number of n to give a approximate solution of critical state. The true critical state, where n equals to infinite is not accessible by FEM software until recently Campbell [28] proposed a novel method of determining critical state which based on the force-displacement curve of the flux lines.

When a force is applied to the flux lines they move elastically for a short distance and then, as they become unpinned, the force becomes a constant frictional force.

$$f = BJ_c(1-\exp(-|s|/d)) \qquad (6)$$

Here f is the force per unit volume; s is the vortex displacement and d a characteristic distance, typically about a quarter of the vortex spacing. The vortex displacement is directly related to the vector potential A [29]. When equation 6 is coupled with equations 1 and 2, it gives:

$$\nabla\times(\nabla\times A) = -sign(A)\mu_o J_c(1-\exp(-|A/Bd|)) \quad (7)$$

Equations 6 can be solved by finite element packages which provide a convenient way of determining the field distribution, losses, and temperature rise in a wide range of superconducting applications. This method gives the critical state directly as a first approximation which avoids some of the numerical difficulty that occur when *E-J* power law is used with a very large number of n, since the relevant power law is $1/n$ rather than n, the solutions are still stable.

5. SUPERCONDUNDCTING MAGNETS

The potential of bulk melt-processed YBCO single domains to trap significant magnetic field at 77K makes them particularly attractive for a variety of engineering applications especially for the applications requiring high field magnets. It has already been shown that large fields can be obtained in single domain samples at 77 K [30, 31]. Machines made using these magnets will be smaller, lighter, and have higher power densities and efficiencies than existing machines. The current record in a disc of diameter 2.65 cm is 17.24 T. This puck on its own could levitate a 6.65 tonne truck! These superconducting bulk magnets are set to revolutionise areas such as wind generation where problems are routinely encountered with the sheer physical size of the generator and unreliability of the gearbox. Using superconducting magnets the generator can be made smaller and the gearbox dispensed with entirely. MHD (Magneto-Hydrodynamic) devices in which tidal power can be harnessed using no moving parts and which can harvest the waste power from turbine exhausts become practical and cheap at these magnitudes of magnetic fields. Electric motors for ship, train and aircraft propulsion, areas where space/weight are at a premium all become smaller and lighter.

In this section of the review, a novel method to produce superconducting high field magnets with bulk YBCO materials will be introduced. This method was recently proposed by Coombs [32] which based on a generic idea of flux pumping scheme. In flux pumping a field is swept across the superconductor in a magnetic wave. This field induces current according to Faraday's law. As long as the direction of motion of the magnetic wave is constant then the current induced will always be in the same sense and successive waves will induce more and more current. Traditionally the magnetic wave would be generated either by physically moving a magnet (a ferrous magnet may be made by stroking it with a permanent magnet) or by an arrangement of coils switched in sequence, such as occurs on the stator of a three-phase motor. Coombs describes a solid state method in which a material which changes magnetic state at a suitable magnetic ordering temperature is heated at its edge and the resultant thermal wave produces a magnetic wave which then magnetizes the superconductor.

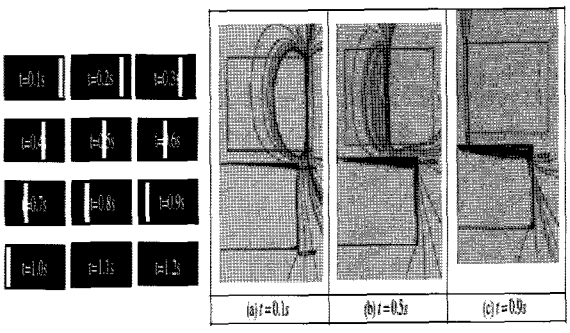

Fig. 8. (a) Magnetic ordering of a switchable material at different time steps. The clear area represents the progression of the magnetic wave. (b) The magnetic wave drags flux across the superconductor and this figure shows the distribution of current and flux density at different time steps in one cycle.

This method is not a classical flux pump as described in Van Klundert et al's excellent review[33]. The method described by Coombs has two unique features. The first is that at no point is the superconductor driven normal; this technique is simply making modifications to the critical state. The second is that the critical state is not modified by a moving magnet or an array of solenoids but by a thermal pulse which modifies the magnetization of a magnetic material thus sweeping vortices into the material. It is a novel kind of heat engine in which thermal energy is being converted into magnetic energy. Figures 8(a) and 8(b) illustrate the process. Figure 8(a) shows the progression of a thermal pulse across a circular puck of magnetizable material. The puck is a ring and the figure shows the right-hand half in cross-section. In figure 8(b) the material depicted in figure 8(a) is shown above a superconducting disc. The figure clearly shows flux being drawn across the surface of the superconductor and the currents which are induced in the superconductor as a result. The method relies on a change in magnetic field due to magnetic ordering/disordering of a material with temperature. There are a range of materials which could be used but the principle is that this technology are looking for a change in magnetization so it prefer to use soft magnetic materials at or near their Curie point. Two suitable soft magnetic materials has been introduced by Coombs: the one can be operated at cryogenic temperatures is the NiII/CrIII analogue of Prussian Blue, Ni1.5[Cr(CN)6] [34]; the other material which can be operated at room temperature is gadolinium, which has unusual property of undergoing a ferromagnetic/paramagnetic transition at around 294 K. This opens up the possibility that the magnetization fixture and the superconductor are physically separated and that measurements can be done with the gadolinium at room temperature and the superconductor cooled by liquid nitrogen. A suitable hard magnetic material to be used as the magnetic source is NdFeB which demagnetizes fairly rapidly but reversibly at cryogenic temperatures.

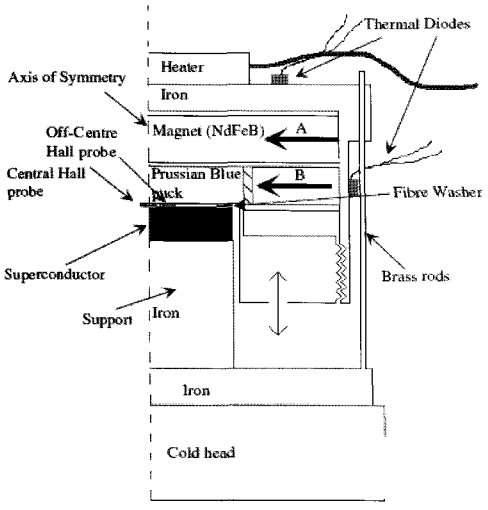

Fig. 9. Cross-section through the right-hand half of the evacuated rig.

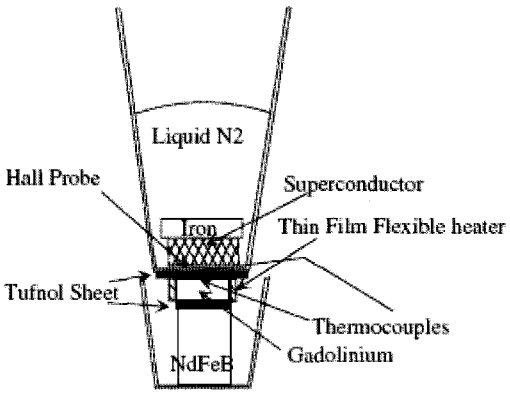

Fig. 10. Experiment rigs.

The principle has been tested in two separate rigs. The first rig which is shown in figure 9 was a fully evacuated rig in which the system was cooled by a cold head. Results are presented for the system using a Prussian Blue analogue as the switching material and also using the variation in magnetization with temperature of NdFeB. A second much simpler system, shown in figure 10, was built where the superconductor is cooled by liquid nitrogen and in this system gadolinium is used as the switching material. The first system was built to investigate the effect of large sweeps and the second system was built to show the effect of multiple small scale sweeps. The two systems both display the same behaviour in that when a heat pulse is applied the net effect is to produce a magnetic wave that travels radially into the centre of the superconductor. In the evacuated rig, cooling was provided by a cold head, warming was provided by conduction and the rig was warmed with the cold head switched off. In the second rig, heating was provided by three 5 W film heaters wrapped around the gadolinium puck. Cooling was provided mostly by conduction from the liquid nitrogen bath in which the superconductor was held. In both systems the principle of operation was the same, that is to achieve a radiating heat/cold flux in the switchable magnetic material which varied periodically and thus induced an associated magnetic wave which traveled radially across the superconductor.

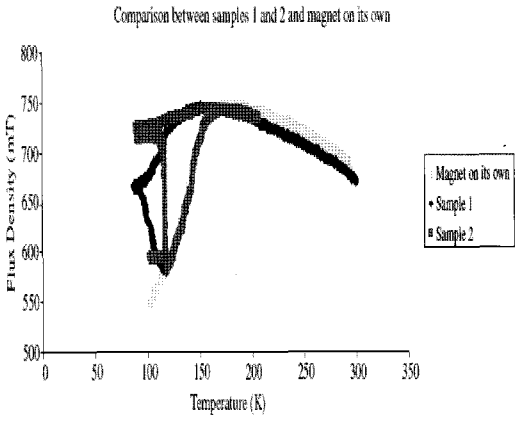

Fig. 11. Magnetisation traces for superconducting samples when the magnet is being cooled then warmed.

Figure 11 shows the results obtained from the evacuated rig when Prussian Blue has been removed and the sample is being swept due to the change in magnetization of the NdFeB with temperature. Only a single cycle is shown for each of the samples but the trace shows clearly the difference in the flux trapping abilities of the two samples. The first sample appears to have been fully penetrated and has trapped about 120 mT while the second sample has trapped about 200 mT. Result in figure 11 demonstrated that it is possible to fully penetrate a sample using this method and that the method works over a small range of cycles and with both hard and soft magnetic materials, the experimentation was moved to the liquid nitrogen rig to investigate the behaviour over a large number of cycles. Fig 12(a) and 12(b)show results from the measurement. Two graphs are given. The first, figure 12(a) shows the overall progression of the magnetic flux density as the system is pumped and figure 12(b) shows a close up section from the data given in figure 12(a). It shows many very small cycles and has been included to illustrate both the fact that the system will continue to accumulate flux after many cycles and that the change per cycle can be controlled so that it is very small, meaning that the final flux density can be very accurately controlled.

This flux pumping technique proposed by Coombs is important for two reasons. The first is that the ability to magnetize superconductors without having to apply large magnetic fields, and with a method which can be easily applied in situ opens up a huge range of potential applications for superconductors as magnets. The second reason is that, although the experiments described herein use a single magnetization fixture, any number of fixtures could be used simultaneously. In other words different parts of the superconductor may be magnetized to a different extent. This means that the overall field profile can beshaped as required.

Consequently the superconducting magnet may be used as an active shim to enhance the field of a conventional solenoid or, as the need arises, to produce large predominantly flat magnets providing highly uniform magnetic fields perpendicular to their surface.

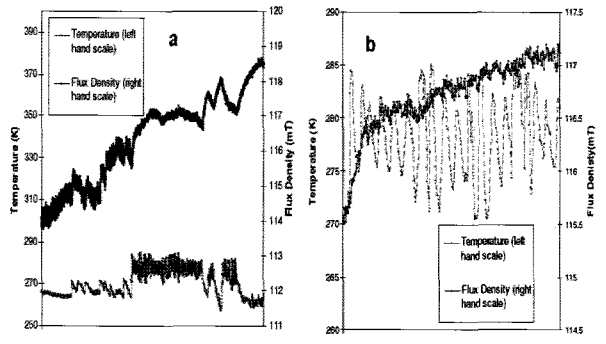

Fig.12. (a) Curve of magnetic induction in superconductor corresponds to the temperature of gadolinium due to many small cycles of pumping. (b) Close up from (a).

6. DEMAGNETISATION EFFECT IN BULK HTS MATERIALS

Before bulk superconductors can be used in the applications of motors and bearings, the characteristics of these trapped field magnets need to be well understood. A major cause for concern is the so-called *crossed field effect*, which is the phenomenon of magnetization decay observed when the material is subjected to magnetic fields in a direction transverse to the original magnetization. This could possibly result in magnets losing their magnetization and thus becoming worthless in applications which exploit the trapped field in HTS materials. In spite of having been investigated for more than three decades, the subject remains a very intriguing topic for which many experimental facts are still far from being understood. In particular we need to know whether large numbers of cycles of the crossed field lead eventually to total demagnetisation or saturates at a useful value.

Early experimental investigations on crossed field configurations involved measuring the magnetic moment of type-II low-T_c superconducting wires subjected to both axial and transverse magnetic fields.[35, 36] Funaki and Yamafuji investigated the behavior of low-T_c materials in the presence of mutually perpendicular DC and AC magnetic fields.[37] In some geometries, the results suggested that the applied AC field suppressed the DC pre-magnetization to varying degrees. Similar effects were observed in high-T_c superconductors, initially for cylindrical YBCO carrying a transport current and subjected to a magnetic field parallel to the cylinder axis[38] and subsequently in high-T_c superconductors of various shapes and microstructures.[39] It is now well-established experimentally that the magnetization M_z of a type-II superconductor sample placed in an external DC magnetic field H_z is decreased strongly by applying a magnetic field H_y perpendicular to both M_z and H_z. This behavior is known as *collapse of magnetic moment*.[40] It has also been observed that subsequent sweeps of the transverse field H_y give rise to further reductions of M_z to a value corresponding to the limiting case for which H_y is an AC magnetic field applied orthogonally to the DC field.

Several theoretical approaches attempt to describe the experimental observations, including the pioneering works of Bean or the double critical-state model of Clem.[39, 41] This model includes the effects of both flux-line pinning and flux-line cutting, i.e. the cross joining of non-parallel vortices at their intersection. In order to further improve the agreement with experimental data, Fisher *et al.* developed a two-velocity hydrodynamic model involving two vortex systems moving at different speeds.[40, 42] This model, however, is limited to small variations of the tilt angle of the total magnetic field, [43] and, as a result, an elliptic flux-line-cutting critical-state model was developed subsequently.[44, 45] In these approaches, the length of the sample is assumed infinite in the direction of both crossed fields, which only arises either for (i) an infinite slab with crossed magnetic fields parallel to the

slab surface or (ii) an infinite cylinder subjected to both azimuthal and axial fields.

The theoretical techniques described above have the common characteristic of assuming a *vertical E-J* characteristic: infinite dissipation is supposed to occur when the critical current components exceed some given value. An alternative approach, proposed by Vanderbemden [46], will be introduced as an example in the review which involves modeling the superconductor with a highly *non-linear E-J* constitutive law $E \propto J^n$, with n being a large number.[17, 47]. Such a relation can be incorporated within the numerical method induced in [11, 12], in which the electric field $\vec{E}$ is always assumed to be parallel to the current density $\vec{J}$. The merit of this work is to validate of the $\vec{E} \parallel \vec{J}$ approach for modeling the results of the crossed field experiments on bulk high-temperature superconductors. Despite its extreme simplicity, this approach will be shown to reproduce successfully many features of the collapse of magnetic moment under transverse fields. In addition to being relevant to several applications of bulk HTS magnets, such geometry will also enable the spatial distribution of the c-axis magnetic flux on the top surface of superconductor to be predicted before and after transverse fields are applied and to compare theoretical predictions to experimental data.

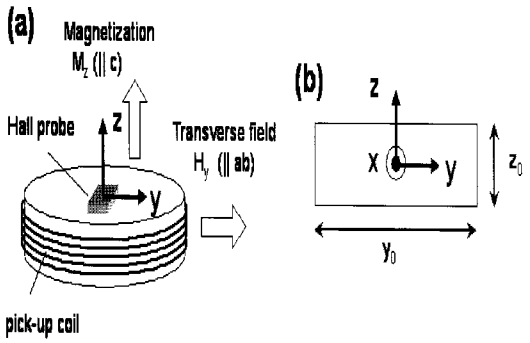

Fig. 13. (a) Schematic illustration of the experimental configuration used for "crossed field" measurements. (b) Geometry used for the two-dimensional model: the sample is of cross-section $y_0 \times z_0$ and is infinite in the x direction.

Bulk melt-textured $YBa_2Cu_3O_{7-x}$ (YBCO) single domains were fabricated by a top seeded melt growth (TSMG) technique [48-50]. In all crossed field experiments, the melt-textured samples were first pre-magnetized parallel to the c-axis by field cooling (FC). The c-axis field was then removed and a constant time interval (two minutes) allowed for magnetic relaxation. A series of transverse magnetic field cycles were then applied parallel to the *ab* plane of the samples. A schematic illustration of the measurement configuration is shown in figure 13. A pick-up coil wound closely around the sample was used to measure the average magnetic properties along the z-axis for sample as described above.

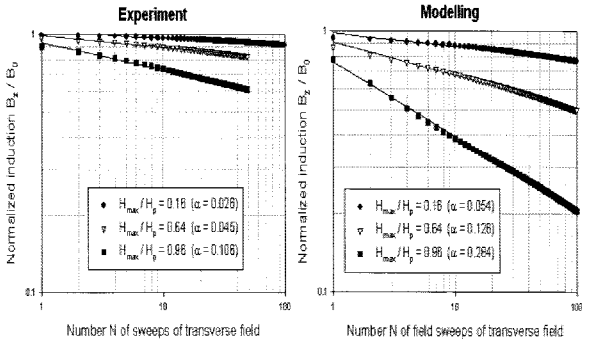

Fig. 14. Log-log plot of the measured and modelled magnetic induction at the end of each transverse field cycle for three different transverse field sweep amplitudes H_{max}.

The influence of a large number of transverse field sweeps on the remanent induction is examined (figure 14). It shows that successive cycles cause the magnetic induction to decrease by smaller and smaller amounts, as illustrated by the log-log plot of the data. The striking feature of figure 14 is that the induction B_z does not appear to saturate, even after a large number of field sweeps. Indeed, the B_z vs. cycle number N curves can be fitted using a power law $B_z \sim N^{-\alpha}$, with the exponent α being an increasing function of the transverse field amplitude H_{max}. Although the study shows that the continuous applying of transverse field leads to a monotonic decay of the trapped magnetic field in superconductors, it doesn't indicate that the superconducting bulk will completely lose the magnetization and lose the potential to be used in rotating machines. It is because in superconducting rotating machines the superconductors used for excitation always see a rotating field instead of a perfect transverse field. The rotating field can be divided into two components, one is orthogonal to the original trapped field; the other is parallel to the original trapped field. The orthogonal component of the rotating field performs the same function as the transverse field mentioned in the pervious paragraph, whilst the parallel components of the rotating field has the potential to partly or fully re-magnetize the sample so that the collapse of the original magnetisation may be less significant or even halted entirely.

Further investigation have been perform by Vanderbemden to verify the maintenance of magnetisation in YBCO bulk when exposed to a rotating external field and promising results have been obtained [51]. Figure 15 shows the remained magnetisation against the number of rotations N for several amplitudes of magnetic field ranging from 0.5 H_p to 2 H_p. The magnetic moment is normalized with respect to its initial value. As can be seen from the figure, the magnetisation decays in the initial cycle of the application of rotating field and increases afterwards. At low amplitudes (0.5 H_p to ~ 0.8 H_p), further rotations yield a monotonic decay of the magnetization whereas at large amplitudes (H_p to 2 H_p), the magnetic moment stabilizes at a plateau whose value is maximum for field amplitudes roughly equal to H_p. There exists an

optimum value and in this experimental condition, a field amplitude of H_p is sufficient to provide a satisfactory remagnetization of the sample.

According to the results presented above, the demagnetization effect in the superconductor can be minimized by optimizing the design of the machines, especially in rotating applications. Even in the situation of superconductor being exposed to a pure transverse field, the demagnetization problem would not be catastrophic either. If the power-law decay behavior holds true, after $N \sim 5\times10^6$ cycles, which would correspond to the application of a 60 Hz AC field for one day, the magnetic induction should reach ~ 68 % of its initial value B_0. A cycle time of more than 422 years would be needed to reach 50 % of B_0. Therefore, bulk superconducting materials have the potential to be an alternative magnetic excitation in electrical devices to produce magnetic field in an order of 5-10 times higher than that of conventional permanent magnets. Successful application of superconducting materials in electrical power system will open a new era in the field of power generation.

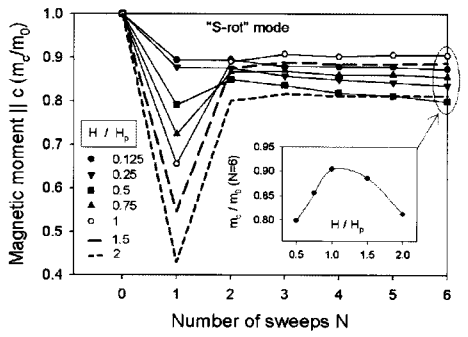

Fig. 15. Measured remained magnetic moment at the end of each rotation cycle for several amplitudes of magnetic field ranging from $0.125\,H_p$ to $2\,H_p$. The magnetic moment is normalized with respect to its initial value m_0.

7. REFERENCE

[1] M. Murakami, *Melt Processed High Temperature Superconductors,* Singapore 1992.

[2] C. K. McMichael, K. B. Ma, M. W. Lin, M. A. Lamb, R. L. Meng, Y. Y. Xue, P. H. Hor, and W. K. Chu, "Effects of material processing in high temperature superconducting magnetic bearings," *Appl. Phys. Lett.* , vol. 59, p. 2442, 1991.

[3] F. C. Moon and P.-Z. Chang, "High-speed rotation of magnets on high Tc superconducting bearings," *Appl. Phys. Lett.* , vol. 56, p. 397, 1990.

[4] H. J. Bornemann, T. Ritter, C. Urban, O. Zaitsev, K. Weber, and H. Rietschel, "Low friction in a flywheel system pith passive superconducting magnetic bearings," *Applied Superconductivity,* vol. 2, pp. 439-447, 1994.

[5] Q. Y. Chen, Z. Xia, K. B. Ma, C. K. McMichael, M. Lamb, R. S. Cooley, P. C. Fowler, and W. K. Chu, "Hybrid high Tc superconducting magnetic bearings for flywheel energy storage system," *Appl. Supercond.*, vol. 9, p. 457, 1994.

[6] T. A. Coombs, A. M. Campbell, I. Ganney, W. Lo, T. Twardowski, and B. Dawson, "Superconducting bearings in flywheels," *Mater. Sci. Eng.*, vol. B, p. 225, 1998.

[7] J. R. Hull, "Flywheels on a roll," *IEEE Spectrum,* vol. 34, pp. 20-25, 1997.

[8] J. R. Hull, T. M. Mulcahy, K. L. Uherka, R. A. Erck, and R. G. Abboud, "Flywheel energy storage using superconducting magnetic bearings," *Applied Superconductivity* vol. 2, pp. 449-455, 1994.

[9] H. Kameno, Y. Miyagawa, R. Takahata, and H. Ueyama, "A measurement of rotation loss characteristics of high-Tc superconducting magnetic bearings and active magnetic bearings," *Applied Superconductivity, IEEE Transactions on,* vol. 9, pp. 972 - 975, 1999.

[10] Y. Miyagawa, H. Kameno, R. Takahata, and H. Ueyama, "A 0.5 kWh flywheel energy storage system using a high-Tc superconducting magnetic bearing," *IEEE Trans. Appl. Supercond.,* vol. 9, p. 996, 1999.

[11] Z. Hong, A. M. Campbell, and T. A. Coombs, "Numerical solution of critical state in superconductivity by finite element software," *Supercond. Sci. Technol. 19 (2006)1246-1252,* vol. 19, pp. 1246-1252, 2006.

[12] Z. Hong, A. M. Campbell, and T. A. Coombs, "Computer Modelling of Magnetisation in High Temperature Bulk Superconductors," *IEEE trans on Applied Science of Superconductor,* vol. 17, p. 3761, 2007.

[13] Y. Jiang, R. Pei, Z. Hong, J. Song, F. Fang, and T. A. Coombs, "Design and control of a superconducting permanent magnet synchronous motor," *Supercond. Sci. Technol.*, vol. 20, pp. 585-591, 2007.

[14] M. Majoros, B. A. Glowacki, A. M. Campbell, G. A. Levin, P. N. Barnes, and M. Polak, "Transport AC losses in striated YBCO coated conductors," *IEEE. Trans. Appl. Supercond.*, vol. 15, p. 2819, 2005.

[15] Y. Jiang, R. Pei, Q. Jiang, Z. Hong, and T. A. Coombs, "Control of a superconducting synchronous motor," *Supercond. Sci. Technol.*, vol. 20, pp. 392-396, 2007.

[16] L. Prigozhin, "Analysis of critical-state problems in type-II superconductivity," *IEEE Trans. Appl. Superconductivity,* vol. 7, pp. 3866-3873, 1997.

[17] E. H. Brandt, "Superconductors of finite thickness in a perpendicular magnetic field: Strips and slabs," *Physical Review B,* vol. 54, pp. 4246-4264, 1996.

[18] E. H. Brandt, "Superconductor disks and cylinder in an axial magnetic field. I. Flux penetration and magnetization curves," *Physical Review B,* vol. 58, pp. 6506-6522, 1998.

[19] E. H. Brandt, "Superconductor disks and cylinder in an axial magnetic field II Nonlinear and linear ac susceptibilities," *Physical Review B,* vol. 58, pp. 6523-6533, 1998.

[20] L. Prigozhin, "Solution of Thin Film Magnetization Problems in Type-II Superconductivity," *Journal of Computational Physics,* vol. 144, pp. 180-193, 1998.

[21] L. Prigozhin, "The Bean Model in Superconductivity: variational Formulation and Numerical Solution," *Journal of Computational Physics,* vol. 129, pp. 190-200, 1996.

[22] G. Barnes, M. McCulloch, and D. Dew-Hughes, "Finite difference modelling of bulk high temperature superconducting cylindrical hysteresis machines," *Supercond. Sci. Technol.*, vol. 13, pp. 229-236, 2000.

[23] G. Barnes, M. McCulloch, and D. Dew-Hughes, "Applications and modelling of bulk HTSs in Brushless ac machines," *Supercond. Sci. Technol.*, vol. 13, pp. 875-878, 2000.

[24] G. Barnes, M. McCulloch, and D. Dew-Hughes, "Computer modelling of type II superconductors in applications," *Supercond. Sci. Technol,* vol. 12, pp. 518-522, 1999.

[25] D. Ruiz-Alonso, T. A. Coombs, and A. M. Campbell, "Numerical analysis of high-temperature superconductors with the critical-state model," *IEEE Trans. Appl. Superconductivity,* vol. 14, pp. 2053-2063, 2004.

[26] T. A. Coombs, A. M. Campbell, A. Murphy, and M. Emmens, "A fast algorithm for calculating the critical state in superconductors," in *COMPEL-The International Journal for Computation and Mathemathics in Electrical and Electronic Engineering*: 20(1):240-252, 2001.

[27] R. Brambilla, F. Grilli, and L. Martini, "Development of an edge-element model for AC loss computation of high-temperature

superconductors," *Supercond. Sci. Technol.* , vol. 20, pp. 16-24 2007.

[28] A. M. Campbell, "A new method of determining the critical state in superconductors," *Supercond. Sci. Technol.,* vol. 20, pp. 292-295, 2007.

[29] B. D. Josephson, "Macroscopic Field Equations for Metals in Equilibrium," *Phys. Rev. A,* , vol. 152, pp. 152-217, 1966.

[30] G. Fuchs, P. Schätzle, G. Krabbes, S. Gruß, P. Verges, K.-H. Müller, J. Fink, and L. Schultz, "Trapped magnetic fields larger than 14 T in bulk $YBa_2Cu_3O_{7-x}$," *Appl. Phys. Lett.,* vol. 76, p. 2107, 2000.

[31] M. Tomita and M. Murakami, "High-temperature superconductor bulk magnets that can trap magnetic fields of over 17 tesla at 29 K," *Nature (London),* vol. 421, p. 517, 2003.

[32] T. A. Coombs, Z. Hong, X. Zhu, and G. Krabbes, "A novel heat engine for magnetizing superconductors," *Supercond. Sci. Technol.,* vol. 21, p. 034001, 2008.

[33] L. J. M. Van de Klundert and H. H. J. Ten Kate, "Fully superconducting rectifiers and fluxpumps Part 1: Realized methods for pumping flux " *Cryogenics,* vol. 21, pp. 195-206, 1981.

[34] M. Tozawa, S. Ohkoshi, N. Kojima, and K. Hashimoto, "Ion-exchange synthesis and magneto-optical spectra of colored magnetic thin films composed of metal(II) hexacyanochromate(III)," *Chem. Commun.,* pp. 1204 - 1205, 2003.

[35] M. A. R. LeBlanc and C. T. M. Chang, "Dependence of the pinning force on magnetic fields in type II superconductors," *Solid State Commun.,* vol. 6, 1968.

[36] M. A. R. LeBlanc and H. G. Mattes, "New Magnetic Phenomenon in Type-II Superconductors," *J. Appl. Phys.,* vol. 41, p. 1567, 1970.

[37] K. Funaki and K. Yamafuji, "Abnormal Transverse-Field Effects in Nonideal Type II Superconductors I. A Linear Array of Monofilamentary Wires," *Jpn. J. Appl. Phys., Part 1,* vol. 21, 1982.

[38] I. V. Baltaga, N. M. Makarov, V. A. Yampol'skii, L. M. Fisher, N. V. Il'in, and I. F. Voloshin, "Collapse of superconducting current in high-T_c ceramics in alternating magnetic field " *Phys. Lett. A,* vol. 148, 1990.

[39] J. L. Giordano, J. Luzuriaga, A. Badía, G. Nieva, and I. Ruiz-Tagle, "Magnetization collapse in polycrystalline YBCO under transport current cycles," *Supercond. Sci. Technol.,* vol. 19, 2006.

[40] L. M. Fisher and et al, "Collapse of the magnetic moment in a hard superconductor under the action of a transverse ac magnetic field," *Physica C ,,* vol. 278, 1997.

[41] C. P. Bean, "Rotational Hysteresis Loss in High-Field Superconductors," *J. Appl. Phys.,* vol. 41, 1970.

[42] L. M. Fisher and et al, "Suppression of the magnetic moment under the action of a transverse magnetic field in hard superconductors," *Phys. Rev. B,* vol. 61, 2000.

[43] J. R. Clem, *Phys. Rev. B,* vol. 26, 1982.

[44] A. F. Caballo-Sánchez, F. Pérez-Rodríguez, and A. Pérez-González, "Magnetic behavior of granular high-Tc superconductors in the weak-link regime," *J. Appl. Phys.,* vol. 90, 2001.

[45] J. R. Clem and A. Pérez-González, "Flux-line-cutting and flux-pinning losses in type-II superconductors in rotating magnetic fields," *Phys. Rev. B,* vol. 30, 1984.

[46] P. Vanderbemden, Z. Hong, T. A. Coombs, S. Denis, M. Ausloos, J. Schwartz, I. B. Rutel, N. H. Babu, D. A. Cardwell, and A. M. Campbell, "Behavior of bulk high-temperature superconductors of finite thickness subjected to crossed magnetic fields," *PHYSICAL REVIEW B* vol. 75, p. 174515, 2007.

[47] N. Amemiya, K. Miyamoto, N. Banno, and O. Tsukamoto, "Numerical Analisys of AC Losses in High Tc Superconductors Based on *E-j* Characteristics Represented with n-Value," *IEEE Trans. Appl. Superconductivity,* vol. 7, pp. 2110-2113, 1997.

[48] R. Cloots, T. Koutzarova, J. P. Mathieu, and M. Ausloos, "From RE-211 to RE-123. How to control the final microstructure of superconducting single-domains," *Supercond. Sci. Technol* , vol. 18, 2005.

[49] J. P. Mathieu, T. Koutzarova, A. Rulmont, J. F. Fagnard, Ph. Laurent, B. Mattivi, Ph. Vanderbemden, M. Ausloos, and R. Cloots, "From RE-211 to RE-123. How to control the final microstructure of superconducting single-domains," *Supercond. Sci. Technol.* , vol. 18, 2005.

[50] N. Hari Babu, M. Kambara, Y. H. Shi, D. A. Cardwell, C. D. Tarrant, and K. R. Schneider, "Processing and microstructure of single grain, uranium-doped Y-Ba-Cu-O superconductor," *Supercond. Sci.*

[51] P. Vanderbemden, Z. Hong, T. A. Coombs, M. Ausloos, N. H. Babu, D. A. Cardwell, and A. M. Campbell, "Remagnetization of bulk high-temperature superconductors subjected to crossed and rotating magnetic fields," *Supercond. Sci. Technol.,* vol. 20, pp. 174-183, 2007.